Title: **Normalization models of cue combination in touch**

Md. Shoaibur Rahman, Jeffrey M. Yau*

Department of Neuroscience, Baylor College of Medicine, Houston, TX 77030 USA

Corresponding author: Jeffrey M. Yau
One Baylor Plaza, T111
Houston, TX 77030
713-798-5150
jeffrey.yau@bcm.edu

Bimanual touch may require combining what is felt on the hands with where the hands are located in space. The computations supporting bimanual touch are poorly understood. We found that tactile cue combination patterns and their sensitivity to the locations of the hands differed according to the attended stimulus feature. These idiosyncratic perceptual patterns can be explained by distinct cue combination models that each involve divisive normalization, a canonical computation.

Mundane tasks like fastening a button or tying shoelaces are possible because of specialized neural circuits for coordinating our use of two hands. Although bimanual movement control has received great attention[1,2], the integrative processing of sensations over the hands remains poorly understood. The somatosensory system uniquely contains a deformable sensory sheet – the relative locations of touch receptors can change depending on the positioning of the limbs and hands – so bimanual touch may require combining what is felt on the hands with where the hands are located in space. Tactile events experienced on one finger can influence how touch on another finger is detected[3–5] or perceived[6,7], and some cutaneous interactions are modulated by proprioception[8,9]. Critically, the computations that support tactile cue combination have not been established. To address this gap, we characterized how subjects discriminate touch under bimanual stimulation and determined whether cutaneous interactions depend on the locations of the hands. We evaluated different models to infer the computations supporting bimanual cue combination.

To characterize bimanual cue combination in the frequency domain, we had participants perform a frequency discrimination task using their right hand as we manipulated the frequency of a distractor cue presented to their left hand and the location of the left hand. While participants maintained high performance levels in all conditions, the distractor cues systematically and reliably altered response patterns despite an explicit instruction to ignore the distractors (**Fig. 1a** and **Supplementary Fig. 1**). The perceived frequency of the 200-Hz target stimulus (**Fig. 1b**) was significantly biased toward distractor frequencies in a manner that depended on distractor hand location. Distractors also significantly altered perceptual thresholds (**Fig. 1c**) in a manner that depended on frequency and hand location. When the target and distractor frequencies differed, distractors induced greater biases in frequency judgments and elevated thresholds more as the hands were located closer in space. When the target and distractor frequencies matched, bias estimates remained unchanged, but thresholds increased with larger separations between the hands. Importantly, merely manipulating hand position without delivering distractor cues did not alter performance (**Supplementary Fig. 2**). These patterns reveal that bimanual cue combination in the frequency domain is obligatory and strongly dependent on target and distractor cue relationships in frequency and space.

To characterize bimanual cue combination in the intensity domain, we had participants perform an analogous intensity discrimination task in which distractor amplitude was manipulated in addition to distractor hand location. If similar bimanual integration rules apply in the frequency

and intensity domains, we predicted that 1) the perceived intensity of a target cue would be biased toward the intensity of the distractor cues, and 2) the magnitude of distractor effects would vary according to hand location. Although distractors systematically and reliably altered the perceived intensity of the target cue (**Fig. 2a** and **Supplementary Fig. 1**), the pattern of distractor effects in the intensity discrimination task clearly differed from the pattern observed in the frequency discrimination task. Distractors only reduced the perceived intensity of target cues (**Fig. 2b**) and attenuation scaled with distractor amplitude. Notably, distractor effects did not vary with hand location (**Fig. 2b**) and distractors exerted no consistent influences on intensity discrimination thresholds (**Fig. 2c**). Thus, although there is also an obligatory interaction between bimanual cues in the intensity domain, the interaction patterns in the frequency and intensity domains differ markedly implying the involvement of distinct neural computations.

To gain insight into the computations supporting bimanual interactions, we tested a number of cue combination models (**Supplementary Table 1**). We noted that the attractive distractor influences in the frequency domain were broadly consistent with linear integration models routinely invoked for multisensory processing[10]; however, the complex effects on thresholds, which depended on both distractor frequency and location, implied additional operations. We performed quantitative comparisons of models (**Supplementary Fig. 3** and **Supplementary Table 2**) that each assumed a weighted combination of the target and distractor cues, but that differed in their treatment of frequency and position manipulations. The most probable model (**Fig. 3a**) was defined by three key components: A frequency-based modulation function that determined the variance of the cue representations, a location-based weighting function that determined the cue weights, and divisive normalization. This model fully recapitulated the observed bias and threshold changes (**Fig. 3b**). On average, the model accounted for 94±1.1% of the variance in split-half cross-validation tests performed on each subject's data (**Fig. 3c**). Moreover, the model explained 96±1% of the variance in across-subject cross-validation tests, approaching the maximum achievable model performance given the measurement noise and inter-subject reliability.

Given their restriction to bias changes and invariance to hand position manipulations, we hypothesized that bimanual intensity interactions were supported by other computations. Distractors only attenuated the perceived intensity of the target cue so their effects could not be explained by linear integration (**Supplementary Table 3**). Intensity interaction patterns were instead consistent with a normalization model (**Fig. 3d**). The pooling for the normalizing factor

explains why increases in distractor intensity result in larger reductions in the perceived intensity of the target cue (**Fig. 3e**). The normalization model accounted for 92±2.2% of the variance in within-subject cross-validation tests and 94±2% of the variance in across-subject cross-validation tests (**Fig. 3f**).

That bimanual interactions are characterized by idiosyncratic patterns when attention is directed to vibration frequency or intensity is perhaps unsurprising given that these features are represented by distinct neural codes in primary somatosensory cortex (S1)[11]. Normalization of rate-encoded intensity signals conceivably underlies the perceptual attenuation of the target cue intensity, as proposed for masking effects on tactile detection[12]. The neural mechanisms underlying the representation and integration of vibration frequency remain more enigmatic. Our results suggest that the reliability of vibration frequency representations are modulated before they are normalized and integrated. This process, which depends on computations of frequency and space, bears clear resemblance to normalization models of attention in the visual domain[13]. Because vibration frequency is represented in the spike timing of S1 cortical populations that phase-lock to vibrations experienced on the skin[11], attention may enhance this temporal code's precision[14] or modulate activity in putative downstream neurons that presumably convert the signals into rate-based representations[15]. These representations could then be integrated through mechanisms analogous to those described for multisensory cue combination, which also involve normalization[16]. Whether cue combination occurs at a particular level in the neuraxis is unclear: Bimanual interactions would appear to implicate higher-order somatosensory regions that contain neurons with bilateral receptive fields, although S1 activity could be modulated and normalized via feedback or lateral connections.

Bimanual interactions that are sensitive to hand location likely involve conjunctive neural coding of cutaneous and proprioceptive signals[17]. The events signaled on the fingers may be maintained in limb-based coordinates regardless of their location in external space and cue combination may be more probable when the hands are held in postures that dominate the statistics of coordinated limb usage. Alternatively, cue combination may occur after the tactile events are remapped to external space[18], independent of limb posture or even the contacted skin region. Results of control experiments support the remapping account, as we observed robust proximity-dependent interaction patterns with the arms crossed and uncrossed (**Supplementary Fig. 4**) and with the distractors presented on the forearm rather than the hand

(**Supplementary Fig. 5**). These results implicate the involvement of posterior parietal regions in bimanual interactions given their critical role in attention and coordinate transformations[19].

Our results reveal obligatory interactions between bimanual sensory cues, the patterns of which differ according to the attended stimulus feature. Despite these differences, which likely reflect distinct neural operations, tactile cue combination in both the frequency and intensity domains involve divisive normalization. These findings reinforce the notion that normalization is a canonical neural computation which appears omnipresent in supporting diverse functions like sensory processing, cue integration, attention, and decision-making[20]. Future studies must address how bimanual sensory processing interacts with and supports dexterous bimanual movements and object perception.

METHODS

Methods, supplementary information and any associated references are available in the online version of the paper.

ACKNOWLEDGEMENTS

This work was performed in the Neuromodulation and Behavioral Testing Facilities of BCM's Core for Advanced MRI (CAMRI). We thank Akshat Patel, Sriparna Sen, and Silvia Convento for help with data collection and Umme Farjana for help with graphics editing. We thank Yau Lab members for helpful discussions and comments on early manuscript drafts. This work was supported by BCM seed funds and the Alfred P. Sloan Research Fellowship.

AUTHOR CONTRIBUTIONS

J.M.Y. and M.S.R. developed the ideas and designed the experiments. M.S.R. collected data with help. M.S.R. and J.M.Y. analyzed data; M.S.R. and J.M.Y. wrote the paper.

COMPETING INTERESTS

The authors declare no competing interests.

REFERENCES

1. Shea, C. H., Buchanan, J. J. & Kennedy, D. M. Perception and action influences on discrete and reciprocal bimanual coordination. *Psychon Bull Rev* **23,** 361–386 (2016).
2. Swinnen, S. P. & Wenderoth, N. Two hands , one brain: cognitive neuroscience of bimanual skill. *Trends Cogn Sci* **8,** 18–25 (2004).
3. Tamè, L., Farnè, A. & Pavani, F. Spatial coding of touch at the fingers: Insights from double simultaneous stimulation within and between hands. *Neurosci. Lett.* **487,** 78–82 (2011).
4. Sherrick, C. E. Effects of double simultaneous stimulation of the skin. *Am. J. Psychol.* **77,** 42–53 (1964).
5. Verrillo, R. T., Gescheider, G. A., Calman, B. S. & Van Doren, C. L. Vibrotactile masking: effects of one- and two-site stimulation. *Percept. Psychophys.* **33,** 379–387 (1983).
6. Kuroki, S., Watanabe, J. & Nishida, S. Integration of vibrotactile frequency information beyond the mechanoreceptor channel and somatotopy. *Sci. Rep.* **7,** 2758 (2017).
7. Craig, J. C. & Qian, X. Tactile pattern perception by two fingers: temporal interference and response competition. *Percept. Psychophys.* **59,** 252–265 (1997).
8. Craig, J. C. The effect of hand position and pattern motion on temporal order judgments. *Percept. Psychophys.* **65,** 779–788 (2003).
9. Bufalari, I., Di Russo, F. & Aglioti, S. M. Illusory and veridical mapping of tactile objects in the primary somatosensory and posterior parietal cortex. *Cereb. Cortex* **24,** 1867–1878 (2014).
10. Fetsch, C. R., DeAngelis, G. C. & Angelaki, D. E. Bridging the gap between theories of sensory cue integration and the physiology of multisensory neurons. *Nat Rev Neurosci* **14,** 429–442 (2013).
11. Harvey, M. A., Saal, H. P., Dammann 3rd, J. F. & Bensmaia, S. J. Multiplexing stimulus information through rate and temporal codes in primate somatosensory cortex. *PLoS Biol* **11,** e1001558 (2013).
12. Brouwer, G. J., Arnedo, V., Offen, S., Heeger, D. J. & Grant, A. C. Normalization in human somatosensory cortex. *J. Neurophysiol.* **114,** 2588–2599 (2015).
13. Reynolds, J. H. & Heeger, D. J. The Normalization Model of Attention. *Neuron* **61,** 168–185 (2009).
14. Recanzone, G. H., Merzenich, M. M. & Schreiner, C. E. Changes in the distributed temporal response properties of SI cortical neurons reflect improvements in performance on a temporally based tactile discrimination task. *J. Neurophysiol.* **67,** 1071–1089 (1992).
15. Saal, H. P., Wang, X. & Bensmaia, S. J. Importance of spike timing in touch: an analogy with hearing? *Curr. Opin. Neurobiol.* **40,** 142–149 (2016).
16. Ohshiro, T., Angelaki, D. E. & DeAngelis, G. C. A normalization model of multisensory integration. *Nat Neurosci* **14,** 775–782 (2011).
17. Kim, S. S., Gomez-Ramirez, M., Thakur, P. H. & Hsiao, S. S. Multimodal Interactions between Proprioceptive and Cutaneous Signals in Primary Somatosensory Cortex. *Neuron* **86,** 555–566 (2015).
18. Yamamoto, S. & Kitazawa, S. Reversal of subjective temporal order due to arm crossing. *Nat. Neurosci.* **4,** 759–765 (2001).
19. Heed, T., Buchholz, V. N., Engel, A. K. & Röder, B. Tactile remapping: From coordinate transformation to integration in sensorimotor processing. *Trends Cogn. Sci.* **19,** 251–258 (2015).
20. Carandini, M. & Heeger, D. J. Normalization as a canonical neural computation. *Nat. Rev. Neurosci.* **13,** 51–62 (2012).

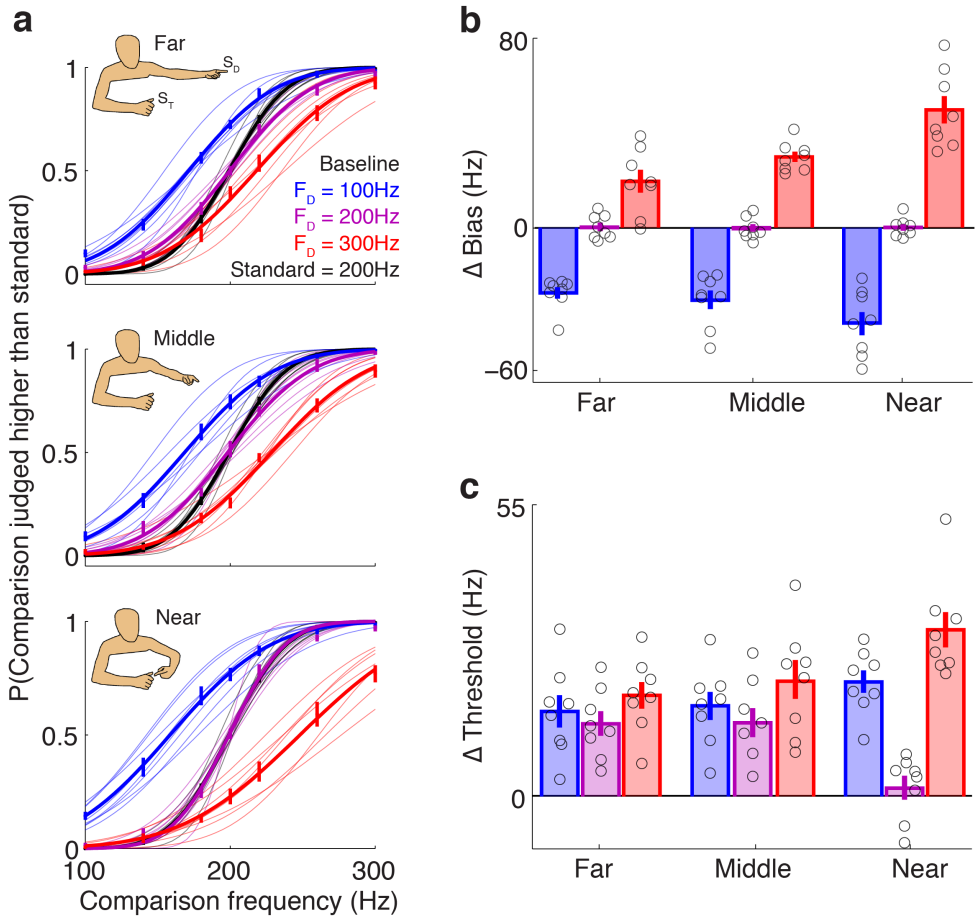

Figure 1 Bimanual interactions in frequency perception. (n = 8) (**a**) Average choice probability and psychometric curves from group (thick traces) and individual subjects (thin traces). Target stimulus (S_T) perception in the presence of distractor stimuli (S_D) differed from perception without distractors (Baseline) depending on distractor frequency (f_D) and distractor hand location. (**b**) Changes in bias (PSE) depended on distractor frequency and location (frequency effect: $F_{2,14}$ = 147.0, P = 4.0e-10, η_p^2 = 0.95; location effect: $F_{2,14}$ = 6.9, P = 0.008, η_p^2 = 0.5; interaction effect: $F_{4,28}$ = 17.8, P = 2.3e-7, η_p^2 = 0.72). Markers indicate individual subjects. Error bars indicate s.e.m. (**c**) Changes in discrimination threshold (JND) depended on distractor frequency and location (frequency effect: $F_{2,14}$ = 12.6, P = 0.0007, η_p^2 = 0.64; interaction effect: $F_{4,28}$ = 12.0, P = 8.6e-6, η_p^2 = 0.63), but the main effect of location failed to achieve significance ($F_{2,14}$ = 0.6, P = 0.55, η_p^2 = 0.08).

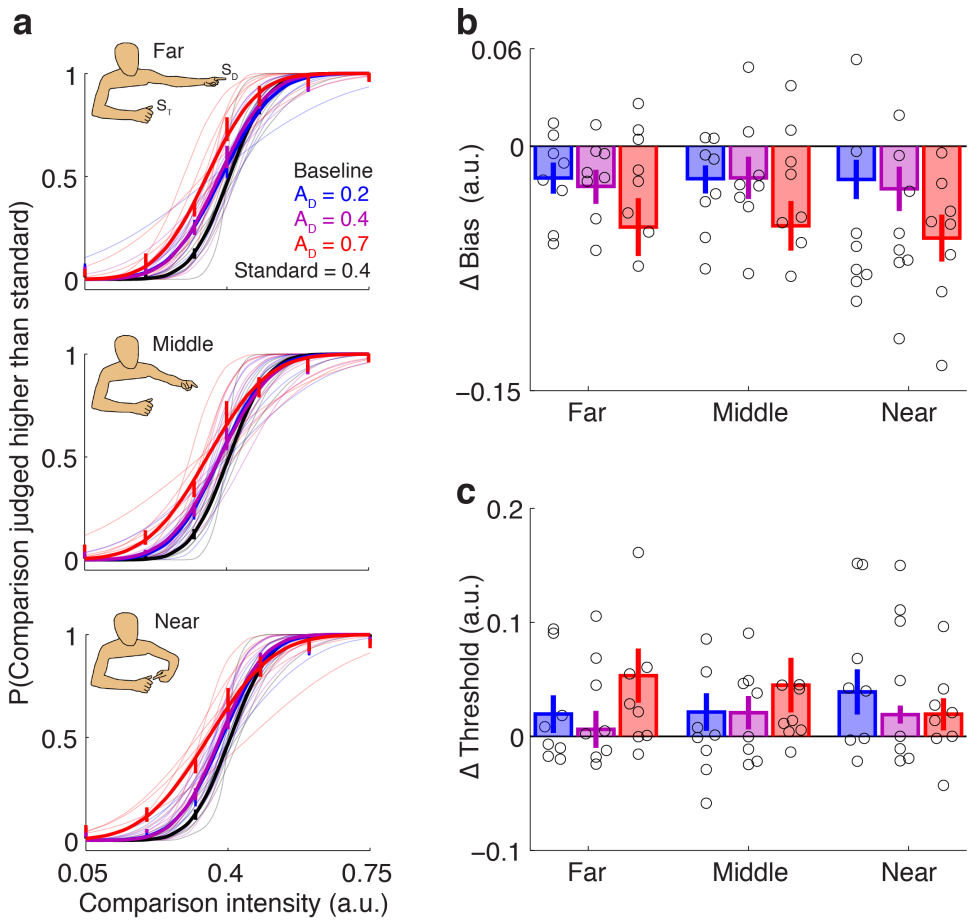

Figure 2 Bimanual interactions in intensity perception (conventions as in **Fig. 1**). (n = 8) (**a**) Average choice probability and psychometric curves from group and individual subjects. Distractors attenuated the perceived intensity of the target stimulus depending on distractor amplitude (A_D). Effects were similar across locations. (**b**) Changes in bias depended on distractor amplitude (amplitude effect: $F_{2,14}$ = 12.4, P = 0.0008, η_p^2 = 0.64), but not distractor location (location effect: $F_{2,14}$ = 0.3, P = 0.74, η_p^2 = 0.04; interaction effect: $F_{4,28}$ = 0.2, P = 0.94, η_p^2 = 0.03). (**c**) No significant changes in discrimination threshold were observed (amplitude effect: $F_{2,14}$ = 1.7, P = 0.23, η_p^2 = 0.19; location effect: $F_{2,14}$ = 0.04, P = 0.96, η_p^2 = 0.005; interaction effect: $F_{4,28}$ = 2.1, P = 0.11, η_p^2 = 0.23).

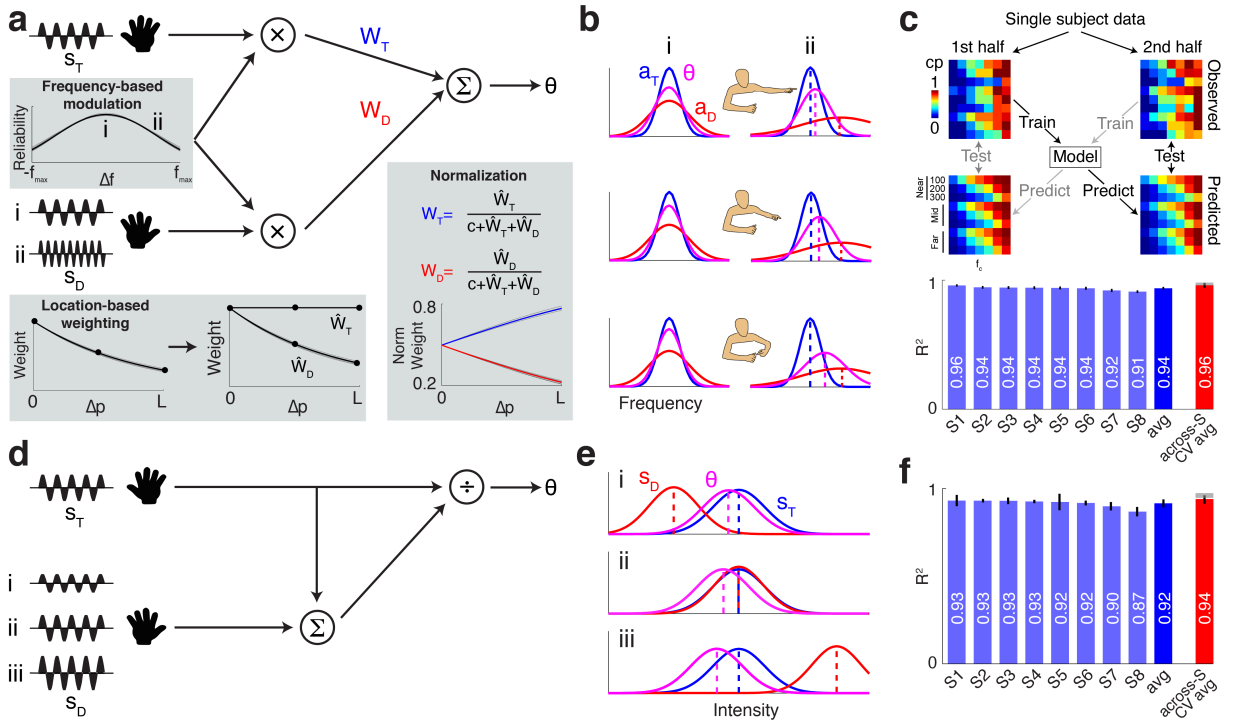

Figure 3 Tactile cue combination models. (**a**) An estimate of the target stimulus frequency (θ) is computed as a linear combination of the target (s_T) and distractor stimulus cues (s_D). Two example distractor frequencies, tested separately in the experiment, are denoted by *i* and *ii*. Cues are modeled by Gaussian probability distributions whose variances are initially set according to baseline discrimination thresholds. A model component capturing frequency-dependent effects (Frequency-based modulation) determines the modulated reliability of each cue according to the frequency disparity (Δf) between the cue and the attended (target) stimulus frequency. A model component capturing the position-dependent effects (Location-based weighting) determines each cue's initial weight ($\widehat{W}_T$ and $\widehat{W}_D$) according to the position disparity (Δp) between the cue and the attended (target) stimulus position (*L* indicates the largest tested separation between the hands). Final target estimates are computed by linearly combining the attention-modulated cue representations using normalized weights (W_T and W_D). (**b**) Plots depict the probability distributions of the attention-modulated cues (a_T and a_D) and the final target estimate under a subset of example distractor conditions. Probability distributions are depicted for different distractor frequencies (columns; corresponding to *i* and *ii* from panel *a*) and relative hand positions (rows). (**c**) Split-half cross-validation was performed within each subject separately. Observed and predicted choice probability (CP) values are shown for an example subject. Blue bars indicate single-subject and group-averaged cross-validated goodness-of-fit. Red bar indicates the average model performance in an across-subject cross-validation procedure. Horizontal gray bar indicates the noise ceiling. Error bars indicated s.e.m. (**d**) An estimate of the target stimulus intensity (θ) is computed from the target (s_T) and distractor stimulus cues (s_D). Three distractor amplitudes, tested separately in the experiment, are denoted by *i*, *ii,* and *iii*. The target cue is normalized by the summed energies of the cues to yield the final target intensity estimate. (**e**) Plots depict the probability distributions of the target and distractor cues (s_T and s_D) and the final target estimate under variations of distractor intensity (*i*, *ii*, and *iii* from panel *d*). (**f**) Model performance from within-subject and across-subject cross-validation procedures. Conventions as in panel *c*.

ONLINE METHODS

Participants. A total of 30 neurotypical subjects participated in at least 1 of 5 experiments. Eight subjects (4m4f; mean age ± standard deviation: 24.5 ± 8.6 years; mean arm length ± standard deviation: 70.8 ± 4.9 cm) performed the main frequency discrimination task (Experiment 1). Eight subjects (3m5f; 22 ± 5.3 years; 67 ± 3.6 cm) performed the main intensity discrimination task (Experiment 2). Eight subjects (3m5f; 21.56 ± 3.9 years; 65.8 ± 3.2 cm) performed the frequency discrimination task in a control experiment with the arm crossing manipulation (Experiment 3). Eight subjects (3m5f; 25.4 ± 5.3 years; 66 ± 3.5 cm) performed the frequency discrimination task in a control experiment in which distractors were delivered to the left forearm (Experiment 4). Eight subjects (2m6f; 22.8 ± 4.6 years; 65.5 ± 3.6 cm) performed the frequency discrimination task on the right hand in a control experiment in which the position of the left hand was manipulated without distractor stimulation (Experiment 5). One subject participated in Experiments 3, 4, and 5; one participated in Experiments 1 and 5; one participated in Experiments 2 and 3; one participated in Experiments 3 and 5; two subjects participated in Experiments 1 and 4; and two subjects participated in Experiments 4 and 5. All subjects were right-handed according to the Edinburgh Handedness Inventory[21]. Testing procedures were performed in compliance with the policies and procedures of the Baylor College of Medicine Institutional Review Board. All participants provided informed written consent and were paid for their participation or declined compensation.

Experiment 1. Frequency discrimination task. Tactile frequency discrimination was tested using a two-alternative forced choice (2AFC) design. On each trial, participants experienced vibrotactile stimulation on their right thumb (target digit, D_T) in two intervals: One interval (randomized over trials) always contained the 200-Hz standard stimulus and the other contained a comparison stimulus whose frequency varied (100, 140, 180, 200, 220, 260, 300Hz). Stimuli were delivered at amplitudes that were equated for perceived intensity[22]. Subjects reported which interval contained the stimulus perceived to be higher in frequency. Participants performed the task in the absence (baseline) and presence of vibrotactile distractors presented to their left index finger (distractor digit, D_D). Subjects were explicitly instructed to ignore the distractor stimuli. On each trial, distractors paired with the comparison stimulus were always matched in frequency. Distractors paired with the 200-Hz standard stimulus were set at 100, 200, or 300Hz. This design enabled us to characterize frequency-dependent distractor influences on the perception of the 200-Hz standard stimulus.

We also manipulated the position of D_D to test whether distractor influences depended on the proximity of the hands. D_T was always positioned 15cm in front the participant's body (midline) with the finger pad facing away from the body. D_D was positioned at three locations (**Supplementary Fig. 6a**): D_D was 1cm from D_T (near position), D_D was co-planar and aligned with D_T as the left arm was fully extended and angled 60° with respect to the body (far position), or D_D was located at the midpoint between the near and

far positions (middle position). Magnetic holders secured the fingers to the table surface ensuring that hand positions and alignments were consistent throughout the experiment. Participants' hands were visually occluded using custom-designed goggles.

Each subject was tested in 2 sessions (inter-session interval: 4.3 ± 4.6 days). Within a session, an equal number of trials were tested under the baseline condition (D_T with no distractor), 9 distractor conditions (3 distractor frequencies x 3 distractor positions), and a condition in which the discrimination task was performed using D_D only. In each condition, the total repetitions of each comparison frequency depended on its absolute difference with respect to 200Hz (Δ100Hz = 10 reps; Δ60Hz = 11 reps; ≤Δ20Hz = 12 reps) to bias sampling to the more challenging comparisons. This yielded 78 trials per condition and 858 trials per session. In each session, baseline trials were randomized and tested in a single block. Trials involving D_D only were similarly tested. Distractor trials were pseudo-randomized according to distractor position. Each distractor position was tested in 3 blocks yielding a total of 9 distractor blocks, the order of which was counterbalanced over subjects and sessions. Subjects were provided 2-3 min between blocks to rest. Over two sessions, this study design yielded 1716 trials per subject.

Experiment 2. Intensity discrimination task. Subjects' ability to discriminate vibration intensity was tested using the same 2AFC procedure as described for Experiment 1. On each trial, participants judged the intensity of tactile stimulus pairs that were delivered to their right thumb. All stimuli were matched in frequency (200Hz) and were clearly suprathreshold. The amplitude of the standard stimulus was 0.4 (arbitrary units). The amplitude of the comparison stimuli varied (0.05, 0.2, 0.32, 0.4, 0.48, 0.6, 0.75). The voltage measured from the amplifier's output ranged from 0.6–3.3V over the tested vibration amplitudes. Subjects performed the intensity discrimination task in the absence and presence of distractors. The amplitude of the distractors, presented to the left index finger, were either 0.2, 0.4, or 0.7. As in Experiment 1, distractor stimuli presented during the comparison stimulus interval always matched the target stimulus experienced on D_T. The position of the distractor digit was manipulated as in Experiment 1. Over two sessions, this study design yielded 1716 trials per subject.

Experiment 3. Frequency discrimination task with arm crossing manipulation. The procedure was similar to that described for Experiment 1 with the major exception that only two limb configurations were tested: Arms uncrossed and crossed (**Supplementary Figs. 4** and **6b**). In the uncrossed configuration, the target digit (right thumb) and distractor digit (left index finger) were positioned 15cm in front of the body to the right and left of midline, respectively. In the crossed configuration, the locations of the hands were reversed such that the right and left hands were positioned to the left and right of midline, respectively. In both configurations, the distance between the target and distractor digits was 20cm. Two distractor frequencies (100 and 300Hz) were tested. This design enabled us to test whether bimanual interactions in the frequency domain were associated with specific limb configurations or simply the

distance between the hands irrespective of limb configuration. Over two sessions, this study design yielded 936 trials per subject.

Experiment 4. Frequency discrimination task with forearm distractors. The procedure was similar to that described in Experiment 1 with the major exception that the distractors were presented on the left forearm rather than the left hand. As in Experiment 1, the target digit was maintained in front of the body at midline and the left arm was repositioned to manipulate the location of the distractor (**Supplementary Figs. 5** and **6c**). In the near position, the stimulated forearm site was 1cm from the target digit. In the far position, the left arm was extended away from the target digit. Two distractor frequencies (100 and 300Hz) were tested. This design enabled us to test whether position-dependent cutaneous interactions in the frequency domain only occur under bimanual stimulation conditions. Over two sessions, this study design yielded 780 trials per subject.

Experiment 5. Frequency discrimination task with manipulations of the distractor hand in the absence of distractor stimulation. The procedure was identical to that described for Experiment 1 except that no distractor stimulation was presented. In this experiment, we only manipulated the position of the left hand (**Supplementary Figs. 2** and **6a**) while subjects performed the frequency discrimination task using their right hand. In a single session, this study design yielded 432 trials per subject.

Vibrotactile stimulation. Sinusoidal signals were digitally generated (sampling rate: 44.1kHz) in Matlab (2011b, MathWorks) running on a Macbook Pro (model A1278; OS X 10.9.5, 2.5GHz Core i5, 4GB RAM)[22]. The experiment was controlled using Psychtoolbox-3. Each 800-ms stimulus was characterized by linear on- and off-ramps (ramp duration: 50ms). Stimuli on each trial were separated by an 800-ms inter-stimulus interval. The signals were outputted via the auxiliary port, amplified (Krohn-Hite Wideband Power Amplifier, model 7500), and delivered to the skin through miniature electromechanical tactors (Fingers: type C-F, Engineering Acoustics, Inc.; Forearm: type C-2, Engineering Acoustics, Inc.). Tactors were fastened to the distal phalanges of the index fingers or the left forearm self-adherent cohesive wrap bandages. Subjects wore earmuffs (Peltor H10A Optime 105 Earmuff, 3M) to attenuate any sounds associated with the tactile stimulation.

Data Analysis. Analyses were performed using Matlab and R-studio. To quantify each participant's ability to discriminate tactile frequency in the baseline and distractor conditions, we fitted each subject's performance data with a Gaussian cumulative distribution function:

$$\mathrm{p}(f_c > f_s) = \frac{1}{2}\left(1 + \mathrm{erf}\left(\frac{f_c - \mu}{\sqrt{2\sigma^2}}\right)\right)$$

where $p(f_c > f_s)$ is the choice probability (CP) indicating the proportion of trials a comparison stimulus with frequency f_c was judged to be higher in frequency than the standard stimulus f_s, μ and σ are free parameters corresponding to the point of subjective equality (PSE) and just-noticeable difference (JND), respectively, and erf(x) is the error function of x. The PSE is a measure of bias and indicates the comparison frequency perceived as equal to the standard frequency. The JND is a measure of sensitivity that is defined as the standard deviation of the Gaussian, which corresponds to 84% performance. Participants' ability to discriminate vibration intensity in Experiments 2 was also quantified using the Gaussian cdf.

In group-level analysis, we determined whether baseline-subtracted PSE and JND estimates differed significantly according to distractor conditions. In Experiments 1–4, we conducted two-way repeated-measures ANOVA (rmANOVA) with frequency (or intensity) and position as the within-subjects factors. In Experiment 5, we conducted a one-way rmANOVA with distractor hand position as the within-subjects factor.

Modeling tactile cue combination. *General*. To understand the computing principles underlying tactile cue combination, we implemented and compared competing models for bimanual interactions in the frequency and intensity domains separately. For each model, we assumed that the nervous system initially represents the target stimulus and distractor stimulus as Gaussian probability distributions $s_T \sim N(\hat{\mu}_T, \hat{\sigma}_T)$ and $s_D \sim N(\hat{\mu}_D, \hat{\sigma}_D)$, respectively. Based on these representations, we assumed that the nervous system computes a final estimate of the target stimulus, $\theta \sim N(\mu_\theta, \sigma_\theta)$. The variances of the initial target and distractor representations were determined empirically in the psychophysical experiments.

Cue combination in the frequency domain. We assumed that the final target estimate is computed as a weighted combination of the target and distractor representations. We also assumed that the weighting of the target and distractor representations as well as their variances (reliability) can be modulated before the final target estimate is computed. Thus, the model takes the general form:

$$\theta = W_T a_T + W_D a_D \tag{1}$$

where, θ is the representation of the final estimate, $a_T \sim N(\mu_T, \sigma_T)$ and $a_D \sim N(\mu_D, \sigma_D)$ are the modulated representations of s_T and s_D, respectively, and W_T and W_D are their respective weights. According to this model, the predicted bias (μ_θ, PSE) and threshold (σ_θ, JND) of the final estimate are determined as:

$$\mu_\theta = W_T \mu_T + W_D \mu_D, \text{ and, } \sigma_\theta = \sqrt{W_T^2 \sigma_T^2 + W_D^2 \sigma_D^2} \tag{2}$$

The most probable model given our data (see *Model selection*) comprised 4 free parameters and included three key functions: frequency-based cue reliability modulation, location-based cue weighting, and normalization. The frequency-based reliability modulation function sets the reliability of each cue representation according to the cue's frequency:

$$M_r(\Delta f) = c_1 \exp\left(-\frac{\Delta f^2}{c_2}\right) \tag{3}$$

where the modulation values in M_r are normally distributed over Δf (the difference in frequency between each cue and the standard frequency), and c_1 and c_2 are free parameters. This component can be considered to reflect feature-based attention directed toward the standard frequency, 200Hz. The function determines the modulated reliabilities of both the target and distractor cues:

$$\sigma_T = \hat{\sigma}_T / M_r(0), \text{ and, } \sigma_D = \hat{\sigma}_D / M_r(\Delta f) \tag{4}$$

Although the modulation function's impact is substantially greater on the distractor representations, the function causes a slight increase in the variance of the target cue representation (Fig. 3b) which is consistent with an attentional cost to ignoring the distractor. Also, because the modulation function only sets the variance of the cue representations, $\mu_T = \hat{\mu}_T$ and $\mu_D = \hat{\mu}_D$.

The location-based weighting function determines the contribution of each cue according to the cue's position:

$$M_w(\Delta p) = \exp\left(-\frac{\Delta p}{c_3}\right) \tag{5}$$

where M_w is exponentially distributed over Δp (the distance between the target and distractor hands) and c_3 is a free parameter. To account for variations in subject arm lengths, the relative distances in the near, middle, and far positions were 0, 0.5, and 1, respectively. This component can be considered to reflect spatial attention directed toward the location of the target hand. Accordingly, before normalization, the target cue is assigned the maximum weight by M_w under all of the limb configurations while the weight to the distractor cue decreases with greater inter-manual separation (Fig. 3a).

The final weights to the target (W_T) and the distractor (W_D) that determine their contributions to the final estimate are computed using a normalization function that includes a single free parameter, c_4:

$$W_T = \frac{M_w(0)}{c_4 + M_w(0) + M_w(\Delta p)}, \text{ and, } W_D = \frac{M_w(\Delta p)}{c_4 + M_w(0) + M_w(\Delta p)} \tag{6}$$

We tested a total of 19 alternative models. All of the models assumed a linear combination of the target and distractor representations (Eqs. 1, 6) but differed in the determination of the target and distractor cue reliabilities and their weights (**Supplementary Table 1**).

Cue combination in the intensity domain. We separately modeled distractor influences on tactile intensity perception, which were limited to changes in bias. The most probable model given our data was one incorporating only divisive normalization: The perceived intensity of the target stimulus (μ_θ) is estimated by normalizing the representation of the target cue amplitude with the sum of the target and distractor cue amplitudes:

$$\mu_\theta = \frac{I_T}{\alpha + \frac{1}{2}(I_T + I_D)} \tag{7}$$

where I_T is the target amplitude, I_D is the distractor amplitude, and α is a free parameter. This model assumes no effects on discrimination thresholds in the intensity domain, so the threshold associated with the final estimate matches the threshold associated with the target cue alone, $\sigma_\theta = \sigma_T$.

We compared the normalization model to an alternative model based on simple cue averaging. In this model, the perceived intensity of the target stimulus is estimated by averaging the amplitudes of the target and distractor cues, again assuming no changes in the perceptual threshold:

$$\mu_\theta = \frac{1}{2}(I_T + I_D), \text{ and } \sigma_\theta = \sigma_T \tag{8}$$

Model fitting and performance assessment. *Single subject fitting*. Model parameters were estimated using a within-subject cross-validation procedure. Each subject's data were divided into two sets that contained an equal number of repetitions for each experimental condition. This pseudo-random data partitioning permitted the calculation of unbiased choice probability values for each split-half dataset. Using two-fold cross-validation, the model was trained on one dataset using maximum likelihood estimation and tested on the second dataset. The squared correlation between the observed and predicted CP was computed as a measure of variance explained for each fold and the variance explained was averaged over both folds for a single goodness-of-fit measure. This two-fold cross-validation procedure was repeated 100 times for each subject.

Group-level fitting. To compare parameter estimates and model performance at a group level, we adopted a leave-one-subject-out cross-validation approach. On each fold, the model was trained on the full datasets of 7 subjects and tested on the data of the held-out subject. The goodness-of-fit calculated in this manner provides an estimate of the inter-subject reliability of the models. Using the same leave-one-subject-out procedure, we calculated the response variance in a single subject explained simply by the

averaged data over the other 7 subjects. The group-averaged data provided a parameter-free model which established a noise ceiling against which we compared the goodness-of-fit values calculated for the fitted models.

We additionally conducted Bayesian analyses to evaluate each candidate model against the parameter-free model established by the leave-one-subject-out cross-validation (**Supplementary Tables 2 and 3**). For each model separately, we quantified the relative support for the alternative hypothesis that the model was outperformed by the parameter-free model (H_1) compared to the null hypothesis of no performance differences (H_0) where the Bayes factor (BF) was $p(data|H_1)/p(data|H_0)$. Thus, smaller BF values indicated stronger evidence for each fitted model.

Model selection criteria. We adopted a number of complementary approaches for selecting a favored model among the alternative models.

Log-likelihood. If an experiment consists of n independent Bernoulli trials, each having probability of success (p) and total number of successes in the trials (x), then the likelihood is:

$$L(p;x) = \frac{n!}{x!(n-x)!} p^x (1-p)^{n-x}$$

Maximizing the likelihood is equivalent to maximizing the log-likelihood $(ll(p;x))$, which is given by:

$$ll(p;x) = \log \frac{n!}{x!(n-x)!} + x \log p + (n-x) \log(1-p)$$

The first term of the above equation is a constant that does not involve the parameter p, where p is expressed as a Gaussian cdf. So, for a given model, we maximize:

$$\begin{aligned} ll(p;x) &= x \log p + (n-x) \log(1-p) \\ &= x \log \left| \frac{1}{2}\left(1 + \operatorname{erf}\left(\frac{f_c - \mu}{\sqrt{2\sigma^2}}\right)\right) \right| + (n-x) \log \left| \frac{1}{2}\left(1 - \operatorname{erf}\left(\frac{f_c - \mu}{\sqrt{2\sigma^2}}\right)\right) \right| \end{aligned}$$

where, μ and σ are the bias and threshold parameters, respectively, estimated for the CP values predicted by the model. The log-likelihood value associated with each model was computed and we favored the model identified with the maximum log-likelihood value.

Residual Sum of Squares (RSS). We computed RSS, the sum of squared errors between the measured data (p) and the data predicted $(\hat{p})$ by the model, as a measure of prediction error. We favored the model with the minimum RSS value.

$$\mathrm{RSS} = \sum_{i} (p_i - \hat{p}_i)^2$$

Akaike Information Criteria (AIC). We computed AIC as a selection measure that balanced model complexity (k, number of estimated parameters) and model performance (L, the maximum likelihood of the model). We favored the model with the lowest AIC value.

$$\mathrm{AIC} = 2k - 2\ln(L)$$

Bayesian Information Criteria (BIC). We computed BIC as another selection measure that balanced model complexity and performance while adjusting for the number of fitted data points (n). As with AIC, we favored the model with the lowest BIC value.

$$\mathrm{BIC} = \ln(n)\,k - 2\ln(L)$$

Likelihood Ratio Test (LRT). We performed LRT calculations of pairwise model comparisons: One model was designated the null model and the other was designated the alternative model.

$$\mathrm{LRT} = -2\log\left(\frac{L_a}{L_0}\right)$$

where L_0 is the likelihood of the observations under the null model and L_a is the likelihood of the observations under the alternative model. We favored the alternative model if LRT was positive and the null model if LRT was negative.

Probability or Akaike weights. Akaike weights are estimated by normalizing the model likelihood such that the relative likelihoods for all models under consideration sum to 1. Hence, these weights can be considered as reflecting the probability or "weight of evidence" in favor of a given model in a fixed set of alternative models[23]. The weight w_i of the ith model is computed as:

$$w_i = \frac{\exp\left(-{}^{\Delta_i}/_{2}\right)}{\sum_{r=1}^{R} \exp\left(-{}^{\Delta_r}/_{2}\right)}$$

where $\Delta_i = \mathrm{AIC}_i - \mathrm{AIC}_{min}$ and AIC_{min} is the minimum of the AIC_i values over the R alternative models. We favored the model with the highest Akaike weight.

Data and Code Availability. The behavioral data (.mat files) and analysis code are available at https://github.com/YauLab/PROPCUT_MSR2018.

References.

21. Oldfield, R. C. The assessment and analysis of handedness: the Edinburgh inventory. *Neuropsychologia* **9,** 97–113 (1971).
22. Convento, S., Rahman, M. S. & Yau, J. M. Selective Attention Gates the Interactive Crossmodal Coupling between Perceptual Systems. *Curr. Biol.* 1–7 (2018). doi:10.1016/j.cub.2018.01.021
23. Burnham, K. P. & Anderson, D. R. Multimodel inference: Understanding AIC and BIC in model selection. *Sociol. Methods Res.* **33,** 261–304 (2004).